The minimum gap on diluted Cayley trees

1986 J. Phys. A: Math. Gen. 19 3903

(http://iopscience.iop.org/0305-4470/19/18/035)

J. Phys. A: Math. Gen. 19 (1986) 3903-3916. Printed in Great Britain

The minimum gap on diluted Cayley trees

R B Stinchcombe, P M Duxbury† and P Shukla‡

Department of Theoretical Physics, University of Oxford, 1 Keble Road, Oxford OX1 3NP, UK

Received 5 February 1986

Abstract. A new order parameter for percolative systems, the minimum gap (x^*), is calculated on diluted Cayley trees. x^* is self-averaging and finite for concentrations p below p_c and zero above. Numerical work (including finite-size scaling) and analytic arguments show that on approaching p_c from below, $x^* \sim \varepsilon/[\ln(1/\varepsilon)+1+\ln(\alpha-1)]$, where $\alpha+1$ is the coordination number of the Cayley tree and $\varepsilon=(p_c-p)/p_c$. The behaviour of x^* as a function of p (for all $p \leqslant p_c$) is calculated in terms of the solution to a transcendental equation, and as $p \to 0$, $x^* \sim 1+\ln\alpha/\ln p$.

1. Introduction

Many properties of percolative systems have been studied in recent years. Examples include dilute magnetism (Stinchcombe 1983), transport in random media (Deutscher *et al* 1983) and the elastic properties of random solids (Kantor 1985). A great deal of insight into these problems is provided by the study of the geometric percolation problem and the backbone topology at p_c (Stauffer 1979, 1985). A natural extension of these works is the study of breakdown problems in random media (for an introduction to the area see Duxbury *et al* (1986a)). One such problem is dielectric breakdown on percolation clusters below p_c. In a recent letter (Duxbury *et al* 1986b) we have introduced a static approximation to the dielectric breakdown problem in random media. The calculation necessitates the introduction of a new order parameter in percolative systems below p_c. This new order parameter, the minimum gap, is studied in detail on Cayley trees in this paper. A brief account of this calculation has been recently reported (Duxbury *et al* 1986b).

To construct a percolative model for dielectric breakdown in quenched random media, consider the square lattice bond percolation problem below p_c. A typical configuration is shown in figure 1(a). Each occupied bond is considered to be conducting, while each vacant bond is an insulator which can withstand a voltage of 1 V. If more than 1 V is applied across a vacant bond, it breaks down and becomes a conductor. If a large enough external voltage is applied across the system (see figure 1(a)), enough of the vacant bonds break down to make the system a conductor. The voltage at which this first occurs is called the breakdown voltage. It is straightforward to give a qualitative phase diagram for this model, by considering the two cases $p=0$ and $p \geqslant p_c$. For $p=0$, the system is composed of insulators only and an external voltage of $V_b = L$ (with L as defined in figure 1(a)) is required to induce dielectric breakdown; while above p_c, $V_b = 0$. The generic phase diagram is then that given in figure 1(b). It is straightforward

† Current address: Serin Physics Laboratory, Rutgers University, Piscataway, NJ 08854, USA.
‡ Permanent address: Physics Department, North Eastern University, Shillong, India 793003.

0305-4470/86/183903+14$02.50

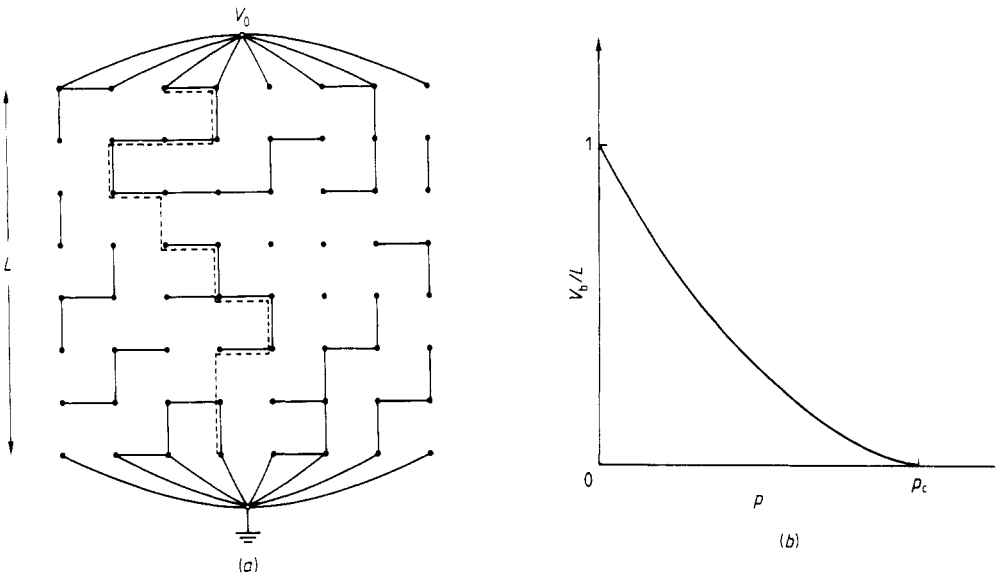

Figure 1. (*a*) The bond percolation problem on a square lattice below p_c. A minimum gap path (going from top to bottom) for this configuration is shown (broken line). The minimum gap is 2. (*b*) The qualitative phase diagram for the breakdown voltage in quenched random media.

to solve the problem in one dimension and in that case $p = 1$ and $V_b = (1-p)L$. The calculation of V_b on regular lattices in $d > 1$ with $0 < p < p_c$ requires the solution to Laplace's equation on the quenched random lattice and the sequential breakdown of any bonds with too much voltage across them. This is a tractable though lengthy numerical process and is at present being undertaken by other workers (Bowman 1985). Preliminary results are consistent with the picture given in figure 1(*b*).

We have instead (Duxbury *et al* 1986b) attempted to construct a simple geometric model that contains some of the essential physics of the dielectric breakdown process. Consider again the model of figure 1(*a*). The basic idea that we use to construct our geometric picture of the breakdown process is to consider that the breakdown paths that eventually occur on increasing the external voltage lie along the paths with the minimum number of vacant bonds. We call these the paths of minimum gap, the total number of missing bonds along them being the minimum gap for that configuration. The breakdown in the model is then simply proportional to his minimum gap. Clearly there are several approximations inherent in this geometric approach (see Duxbury *et al* (1986b) for a discussion). Nevertheless these ideas lead to a qualitatively (and perhaps quantitively) correct estimate of the breakdown voltage and should contain the essential features of the original dielectric breakdown problem.

The problem is still a very difficult one. The minimum gap g is a random variable and so it will be necessary to consider its distribution $P(n, g)$ in a system of size n. In the large system limit $n \to \infty$, where the system is expected to become self-averaging, the system will exhibit the percolation transition, since the probability of zero minimum gap is the order parameter for percolation and is zero (or non-zero) for $p \leqslant p_c$ (or $p > p_c$). Apart from the ordinary critical phenomena of percolation there is critical behaviour of other quantities contained in the minimum gap distribution, of which the principal one, with which we are here mainly concerned, is the average minimum

gap. This quantity is expected to have a behaviour very like that described above for the breakdown voltage, and (when properly normalised) is another order parameter for the problem. The minimum gap is likely to be as difficult to treat as the percolation conductivity, or diffusion, and so on.

As a contribution towards the understanding of this quantity, we here consider the minimum gap on diluted Cayley trees. Cayley trees (Fisher and Essam 1961) provide a non-trivial percolation threshold (unlike the linear chain) and have been very useful in providing the mean-field critical exponents for problems such as percolation conductivity (Stinchcombe 1974, Straley 1977). Such problems are still far from trivial, the latter, for example, involving the scaling solution of a non-linear integral equation for the conductance distribution function. It will be seen in §2, where the model is fully introduced, that the minimum gap problem on diluted Cayley trees involves a non-linear difference equation in two variables (g and n). Numerical investigations of this equation are described in § 4. The results give the nature of the minimum gap distribution for various concentrations (above and below the percolation threshold) and show that the minimum gap is extensive (of order n) for $p < p_c$ and of order 1 for $p \geq p_c$. This suggests using the large system limit of the normalised minimum gap g/n as an order parameter. Numerical results also strongly suggest that this 'reduced minimum gap' vanishes linearly as p tends to p_c from below, with the possibility of, e.g., logarithmic corrections. Section 4 provides an analytic treatment of the properties of the minimum gap. Using procedures suggested by the insight gained from the numerical data in the large system limit, a solution is found for the minimum gap in the large system limit. This solution is in close agreement with the numerical results: it confirms the numerical result for the critical exponent describing the vanishing of the minimum gap and shows that there are logarithmic corrections. It also describes an unexpected feature seen in the numerical results for the gap at very low concentrations. The results and implications are further discussed in § 5.

2. The model

The system geometry is depicted in figure 2(a) for a Cayley tree with coordination number $z = 3$. Each bond may be present or absent with probability p or $(1-p)$. The parameter n labels successive levels on the tree. Each vertex at level n has $z-1 \equiv \alpha$ subtrees incident from below. Let $P(n, g)$ denote the probability that the minimum gap from bottom to top (i.e. level n) across such a subtree is g. Clearly

$$P(0, g) = \delta(g) \tag{1}$$

$$\sum_{g=0}^{\infty} P(n, g) = 1 \tag{2}$$

from 'no gap at level zero' and normalisation, respectively. Though $P(n, g)$ is the distribution function of interest to us, it is convenient to work in terms of the related quantity,

$$U(n, g) = \sum_{g'=g+1}^{\infty} P(n, g') \qquad (g \geq -1). \tag{3}$$

From (1) and (2) above, $U(n, g)$ must satisfy

$$U(0, g) = \delta(g+1) \tag{4}$$

$$U(n, -1) = 1. \tag{5}$$

$U(n, g)$ is the probability that the minimum gap is greater than g 'at level n'. $U(n, g)$ and $P(n, g)$ are both functions of the bond concentration p as well as n and g.

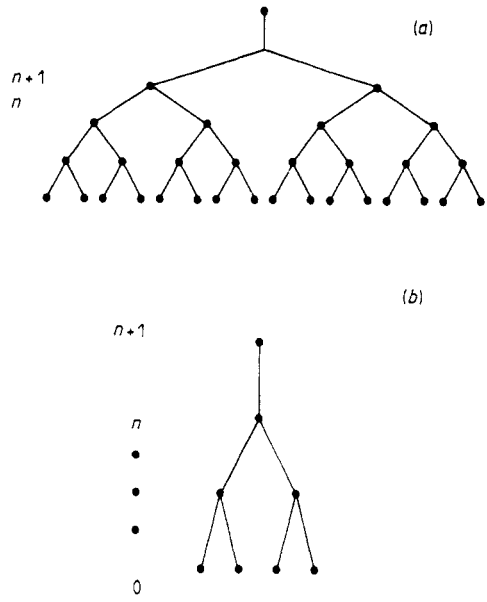

Figure 2. (*a*) The $\alpha = 2$ Cayley tree. (*b*) The labelling system used in the analysis.

The simplifying feature of the Cayley tree model is the statistical independence of the outward branches (because of the absence of closed loops). Moreover, it can be described by recursion relations in the following manner, which relate the properties at successive levels. For the tree shown in figure 2(*a*), consider the subtree shown in figure 2(*b*) which is sufficient to discuss for level $n+1$ the probability $U(n+1, g)$ of minimum gap being greater than g. We consider in turn the cases in which the top bond in figure 2(*b*) is present (probability p) and absent (probability $1-p$). In the first case the minimum gap at $n+1$ is greater than g if the α subtrees incident at n all have minimum gap greater than g. In the second case the minimum gap at $n+1$ is greater than g if all the α subtrees incident at n have minimum gap greater than $g-1$. Adding the probabilities of these two exclusive events gives

$$U(n+1, g) = p[U(n, g)]^{\alpha} + (1-p)[U(n, g-1)]^{\alpha} \qquad (n, g \geqslant 0). \tag{6}$$

This is the fundamental equation of this paper. It is a non-linear recursion in two variables n, g. By iterating it out from (4) and (5) to an appropriate value of n it gives, in principle, the distribution from the minimum gap across a full tree of type shown in figure 2(*a*). Unfortunately, the complete analytic treatment of such an equation is impossible, as the intricacies of better known non-linear iterative maps make obvious (see, for example, Schuster 1985).

It is, however, easy to extract the percolation transition from (6), by considering the special case $g = 0$. For this special case (6) becomes, using (5),

$$U(n+1, 0) = p[U(n, 0)]^{\alpha} + (1-p) \tag{7}$$

which is now a one-variable map. The further discussion of (7) will be continued for the case $\alpha = 2$, which is algebraically simple though it retains the essential features of

the general case. For $\alpha = 2$, the map (7) has fixed points at

$$U^*(0) = 1, (1-p)/p. \tag{8}$$

For $1-p < p$ both fixed points are physically accessible ($U(n, g) \leqslant 1$) and, under iteration in the direction $n \to n+1$, the fixed points being relatively unstable, stable, $U(n, 0)$ converges for $n \to \infty$ towards the attractive fixed point value $(1-p)/p$. For $(1-p) > p$ the second fixed point is unphysical, but the first fixed point is attractive so $U(n, 0) \to 1$. The two situations correspond to being on either side of the percolation transition since the resulting thermodynamic limit ($n \to \infty$) is ($\alpha = 2$)

$$\begin{aligned} U(\infty, 0) &= 1 \qquad && p < p_c = \tfrac{1}{2} \\ &= (1-p)/p \qquad && p > p_c. \end{aligned} \tag{9}$$

Further,

$$1 - U(\infty, 0) = P(\infty, 0) \tag{10}$$

is an appropriate order parameter (the probability of zero minimum gap). For general α, the change in stability of the fixed points occurs at the percolation threshold

$$p = p_c = 1/\alpha. \tag{11}$$

However, the second fixed point in (8), and hence the value in (9) of $U(\infty, 0)$ for $p > p_c$, is now replaced by the solution of an equation of order α.

The behaviour of $U(n, 0)$ at large n (i.e. the finite-size effects) can be obtained by linearising around the stable fixed point $U(\infty, 0)$. In this way, it can be easily shown that the convergence of $U(n, 0)$ to $U(\infty, 0)$ is like

$$U(\infty, 0) - U(n, 0) \sim C(p)\{p\alpha[U(\infty, 0)]^{\alpha-1}\}^n \tag{12}$$

at large n, where $C(p) \approx U(\infty, 0)$. For $p < p_c$, (12) becomes $C(p/p_c)^n$ and in general the convergence with n is extremely rapid, except near $p = p_c$ where it goes like $\exp(-n/\xi)$ with ξ the percolation correlation length.

Further analytic investigation of (6) is more complicated and is deferred until § 4, following the next section in which the results of a numerical attack are presented, which provide an insight into the later analysis.

3. Numerical calculations

It is straightforward to perform a direct iteration of (6) to high order. The calculations need only be monitored to ensure that loss of precision due to round-off error does not occur to a significant degree. The results of a direct iteration of (6) to order 50 are presented in figure 3 for several values of p and $\alpha = 2$. The results for different α are qualitatively similar. The striking feature of figure 3 is the narrow range of g over which the function $U(n, g)$ changes from a value which is very close to 1 to a value which is very close to 0. This crossover region occurs for $p \leqslant p_c$ at $g \sim g^* \propto n$. Since in this p region g^* is extensive, it is appropriate to use

$$x = g/n \tag{13}$$

as the scaling variable. The sharp crossover in $U(n, g)$ is reflected directly in the

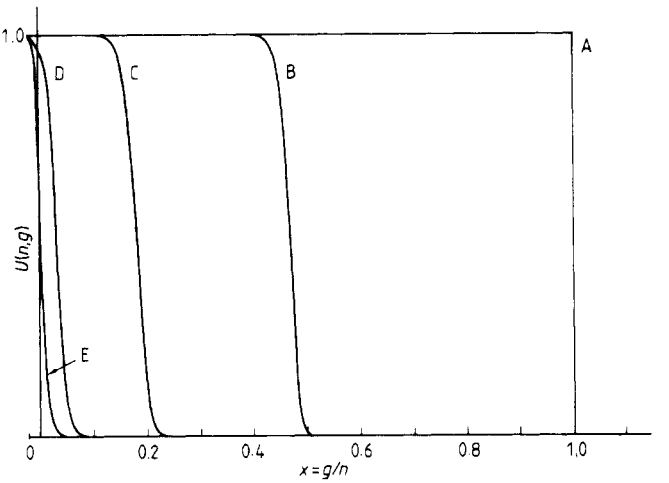

Figure 3. Numerical results for $U(n, g)$ against g/n from the iteration of (6) to $n = 50$, for various values of p. A, 0; B, 0.1; C, 0.3; D, 0.5; E, 0.7.

probability $P(n, g)$ defined by

$$P(n, g) = U(n, g-1) - U(n, g). \tag{14}$$

$P(n, g)$ is sharply peaked at g^*. This is an indication of the fact that the minimum gap is self-averaging even on a Cayley tree. $x^* \equiv g^*/n$ is then essentially an order parameter for $p \leqslant p_c$ and is non-zero for $p \leqslant p_c$ and zero for $p > p_c$.

For $p > p_c$, $U(n, g)$ converges rapidly with n to an n-independent limit $U(\infty, g)$ (thus the g with appreciable probability are order 1), and hence the probability distribution for $x = g/n$ is zero for $x \neq 0$ in the thermodynamic limit. This is another statement of the fact that, for $p > p_c$, $x^* = 0$.

In the numerical calculations it is more convenient to use the average minimum gap defined by

$$\bar{g}(n) = \sum_{g=0}^{n} gP(n, g). \tag{15}$$

This quantity then becomes g^* in the thermodynamic limit. Results for $\bar{x} = \bar{g}/n$ for finite systems are shown in figure 4 for various values of p. The curves converge rapidly with the level number n and an $n \to \infty$ extrapolation indicates that x^* behaves as an order parameter should as $p \to p_c$, vanishing continuously as follows:

$$\bar{x}(\infty) \sim (p_c - p)^{\mu} \tag{16}$$

which defines the critical exponent μ. The other marked feature of figure 4 is the steep approach to $\bar{x} = 1$ as $p \to 0$. This is very different from the linear approach that one might have expected and is further elucidated in the analytical calculations of the next section. Before proceeding to that work we calculate the critical exponent μ appropriate to x^* $(= \bar{x}(\infty))$ near p_c.

In the standard finite-size scaling viewpoint, the order parameter x behaves as

$$\bar{x}(n) = \bar{g}/n = \xi_c^{-\mu/\nu} \Phi(\xi/n) \tag{17}$$

for $n, \xi_c \to \infty$, where

$$\xi_c \sim (p_c - p)^{-\nu} \tag{18}$$

is the chemical distance. The usual crossover scaling argument implies that, at $p = p_c$,

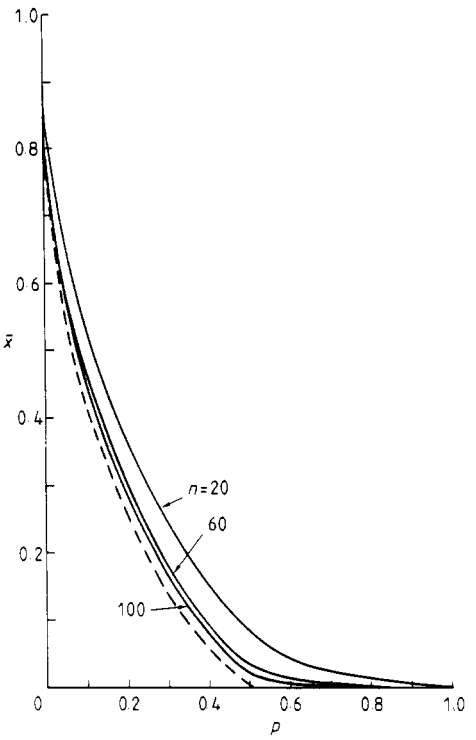

Figure 4. Numerical results for $\bar{x}$ for several values of n. The dotted line is the infinite limit extrapolation.

one has

$$\bar{x}(n) \sim n^{-\mu/\nu}. \tag{19}$$

In the case of the Cayley tree, $\nu = 1$.

Plots of the numerical data for $\bar{x}$ against $1/n$ at $p = p_c$ for $\alpha = 2$ and 8 are presented in figure 5. The large n behaviour is found to be independent of α and the curves are linear up to logarithmic corrections. Using (18), with the Cayley tree value of ν, leads to

$$\mu = 1. \tag{20}$$

Using the general picture obtained from the above analysis we now construct analytic methods to study the problem.

4. Analytic treatment

Although it is impossible to solve (6) exactly for general g, n, it is possible to obtain the thermodynamic limit and to explain the numerical results given in the previous section.

Let us suppose that $U(n, g)$ possesses a well defined thermodynamic limit ($n \to \infty$) $U(\infty, g)$. The numerical results already show that this is the case for $p \leqslant p_c$, but it is

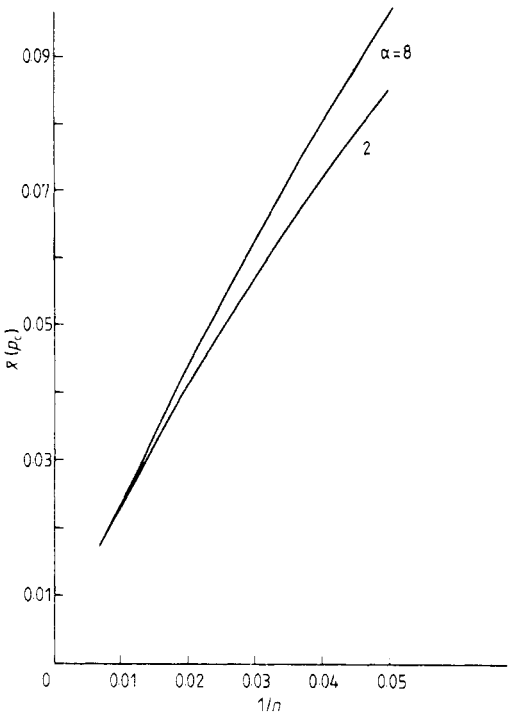

Figure 5. Numerical results for $\bar{x}(p_c)$ against $1/n$ for two values of α. $p = p_c$.

anyway instructive to see how this arises within an analytic discussion. If the assumption is permissible, it is only necessary to consider $U(\infty, g)$ or, equivalently,

$$V(g) \equiv [U(\infty, g)]^{\alpha}. \tag{21}$$

Then from (5) and (6), $V(g)$ satisfies

$$V(g-1) = \{[V(g)]^{1/\alpha} - pV(g)\}/(1-p) = f(V(g)) \tag{22}$$

$$V(-1) = 1 \tag{23}$$

and, since V is the αth power of a probability, it lies in the interval $[0, 1]$.

(22) is a single-variable non-linear iterative map, shown in figures 6(*a*), (*b*) and (*c*) for the three cases $p > p_c = 1/\alpha$, $p = p_c$ and $p < p_c$ respectively. The map function $f(V)$ has the forms shown in the figure because $V = 0$ and $V = 1$ are fixed points of the map, and

$$f'(1) = (p_c - p)/(1-p) \tag{24}$$

so the slope of f at $V = 1$ is positive or negative depending on whether p is less than or greater than p_c. The physical range is the interior of the unit square in the figures.

Case (i) $p > p_c$. For the regime $p > p_c$ successive mappings from $V(-1)$ (unity, according to (23)) to $V(0)$, to $V(1)$, etc, can be carried out by following the zig-zag curve in figure 6(*a*) in the direction of the arrow. The successive values of $V(g)$ fall rapidly from 1 in just the way already demonstrated in the numerical results for $U(n\,g)$ against g at $p > p_c$ in figure 3. The tail of the distribution can be obtained as follows. Once g is such that $V(g)$ is sufficiently small, $f(V)$ can be approximated by $V^{1/\alpha}(1-p)^{-1}$.

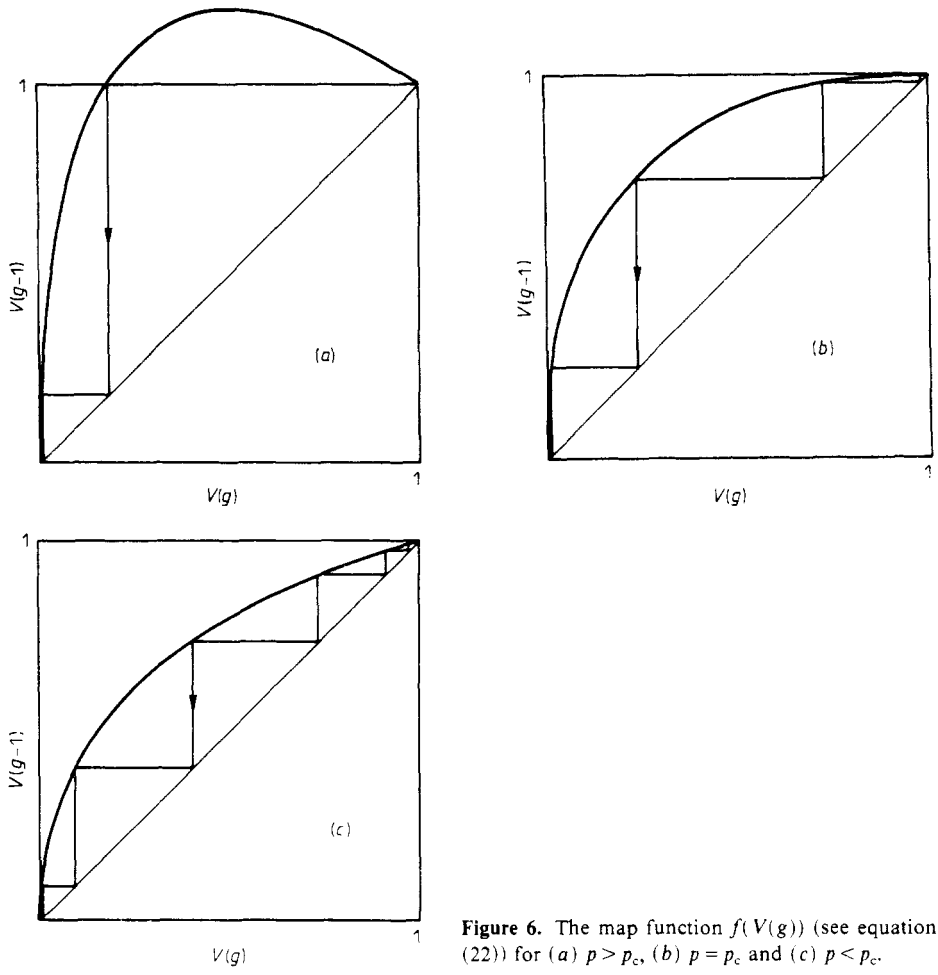

Figure 6. The map function $f(V(g))$ (see equation (22)) for (*a*) $p > p_c$, (*b*) $p = p_c$ and (*c*) $p < p_c$.

Subsequent iterations (increasing g by 1 at each step) then simply multiply $\ln[V(1-p)^{\alpha/(\alpha-1)}]$ by α at each step, so

$$V(g) \sim (1-p)^{-\alpha/(\alpha-1)} \exp[-\alpha^g L(p)] \tag{25}$$

for all g such that $V(g)$ is sufficiently small. $L(p)$ is a g-independent positive quantity which can be obtained by matching (25) to the value of $V(g)$ at the lowest g for which $V(g)$ is sufficiently small to make (25) applicable. For $p > p_c$ such g are of order 1 or 2 except near p_c. The essential point is that for $p > p_c$ an n-independent thermodynamic limit is consistently obtained within this analytic framework and in the numerical work.

Case (ii) $p \leqslant p_c$. However, for $p \leqslant p_c$ the n-independent one-variable iterative map approach breaks down because the initial condition (23) starts the mapping at a place from which no escape is made in a finite number of iterations. Though this is strictly correct (since $\lim_{n\to\infty} U(n, g) = 1$ if g is held finite) and related to the plateau behaviour seen in the numerical results for $U(n, g)$, it does not help us to obtain an overall picture of $U(n, g)$ at large n, whose structure occurs over a range of g proportional to n, according to the numerical work. It is essential to retain the n dependence in (6) to set the scale of the g dependence if $p \leqslant p_c$. Nevertheless, the tail region ($V \ll 1$)

can again be treated as before, and again has the form (25) except that in this case ($p \leqslant p_c$), the matching quantity $L(p)$, while remaining g-independent, is n-dependent (proportional to $\alpha^{-g^*(n)}$, where g^* is defined in § 3 and immediately below) even for large n, and is therefore not accessible within the approach given so far.

A treatment of (6) for the regime $p < p_c$, retaining the n as well as the p dependence, is therefore required. The non-linearity of (6) makes a complete treatment impossible. However, a linearised approach based on the following considerations will lead to the complete thermodynamic limit. According to the numerical work, $U(n, g)$ is very close to 1 in the plateau region extending out to $g = g^* \propto n$, at which $U(n, g)$ turns down rather abruptly. It will turn out from the subsequent analysis that in the large n limit $U(n, g)$ is arbitrarily close to 1 in the plateau region, so that linearisation in

$$f(n, g) \equiv 1 - U(n, g) \tag{26}$$

is valid there, and that it then drops by a finite (n-independent) fraction of its plateau value as g/n increases by $O(1/n)$ beyond the 'edge' ($g/n = O(1)$) of the plateau, moving into the tail which (by (25)) decays over a further increase of g/n by $O(1/n)$. Thus in the thermodynamic limit, U is a step function in the reduced variable g/n, and the edge of the step can be located by determining where the linearisation in f begins to break down.

The linearised approach is now presented. The recursion equation resulting by writing (6) in terms of f, using (26), and discarding powers of f higher than the first is

$$f(n+1, g) = p\alpha f(n, g) + \alpha(1-p) f(n, g-1) \qquad n, g \geqslant 0. \tag{27}$$

The boundary conditions corresponding to (4) and (5) are

$$f(0, g) = 1 - \delta(g+1) \tag{28}$$

$$f(n, -1) = 0. \tag{29}$$

It is convenient to introduce the generating function

$$F(t, g) = \sum_{n=0}^{\infty} f(n, g) t^n. \tag{30}$$

Because of (29),

$$F(t, -1) = 0. \tag{31}$$

Multiplying (27) by t^n and summing over n from 0 to ∞ gives

$$(F(t, g) - f(0, g))/t = p\alpha F(t, g) + \alpha(1-p) F(t, g-1) \qquad g \geqslant 0 \tag{32}$$

or, using (28) and noting that $g \geqslant 0$,

$$(1/t - p\alpha) F(t, g) = \alpha(1-p) F(t, g-1) + 1/t \qquad g \geqslant 0. \tag{33}$$

The form

$$F(t, g) = A(t)[\gamma(t)]^g + a(t) \qquad g \geqslant -1 \tag{34}$$

solves this one-variable linear difference equation, provided

$$\gamma(t) = [\alpha(1-p)t]/(1-p\alpha t) \tag{35}$$

$$a(t) = 1/(1-\alpha t). \tag{36}$$

$A(t)$ is then determined by the boundary condition (31), so

$$F(t, g) = \{1 - [\alpha(1-p)/(1-p\alpha t)]^{g+1}\}/(1-\alpha t). \tag{37}$$

The coefficient of t^n in the expansion of this gives $f(n, g)$, by virtue of (30). The coefficient is easily obtained since

$$F(t, g) = \sum_{r=0}^{\infty} (\alpha t)^r \left(1 - [\alpha(1-p)t]^{g+1} \sum_{s=0}^{\infty} \frac{(g+s)!}{s!\,g!} (p\alpha t)^s\right). \tag{38}$$

Thus

$$f(n, g) = \alpha^n \qquad g \geqslant n \tag{39}$$

$$f(n, g) = \alpha^n (1-p)^{g+1} \sum_{s=n-g}^{\infty} \frac{(g+s)!}{s!\,g!} p^s \qquad g < n. \tag{40}$$

(39) should be discarded, since it is outside the regime in which the linearisation procedure used to get it is valid. The awkward sum (40) can be replaced as follows by an integral in the thermodynamic limit in which g and n are comparably large:

$$I \equiv \sum_{s=n-g}^{\infty} \frac{(g+s)!}{g!\,s!} p^s \tag{41}$$

$$= \int_{n-g}^{\infty} \mathrm{d}s \exp[\ln(g+s)! - \ln g! - \ln s! + s \ln p + \mathrm{O}(1)]. \tag{42}$$

Using Stirling's approximation for the factorials and making the change of variables to $y = s/n$ and

$$x \equiv g/n \tag{43}$$

gives

$$I = n \int_{1-x}^{\infty} \mathrm{d}y \exp[nh(y) + \mathrm{O}(1)] \tag{44}$$

where

$$h(y) = (x+y)\ln(x+y) - x \ln x - y \ln y + y \ln p. \tag{45}$$

Since n is large, a Laplace method can be used to evaluate the integral (44), which is dominated by the contribution coming from the vicinity of a maximum stationary point of $h(y)$ or an endpoint of the interval of integration. It is easy to check that $h(y)$ has a maximum stationary point at $y = px/(1-p)$ lying within the integration interval if $(1-p) < x$. However, if $1-p > x$, the largest value of $h(y)$ is at the endpoint $y = 1-x$. It is not consistent to take $(1-p) < x$, which results in $f(n, g) \sim \alpha^n$ (violating the linearisation assumption). Taking $(1-p) > x$ gives

$$I = \exp[nh(1-x) + \mathrm{O}(1)]/|h'(1-x)| \tag{46}$$

$$= \exp(n\{(1-x)\ln[p/(1-x)] - x \ln x\} + \mathrm{O}(1)). \tag{47}$$

Hence using (40) and (41):

$$f(n, g) = \exp(n\{(1-x)\ln[p/(1-x)] + x \ln[(1-p)/x] + \ln \alpha\} + \mathrm{O}(1))$$

provided

$$x = g/n < (1-p). \tag{48}$$

The exponent in (48) changes sign, from negative to positive, as x increases through $x^*(p)$ where

$$(1-x^*)\ln[p/(1-x^*)]+x^*\ln[(1-p)/x^*]+\ln\alpha = O(1/n). \tag{49}$$

Since the exponent is also proportional to n, the statements made when introducing (26) all follow. In particular, in the thermodynamic limit, $U(n, g)$ becomes the following step function:

$$\lim_{n\to\infty} U(n, nx) = \theta(x^*(p)-x). \tag{50}$$

From (13) it follows therefore that in the regime $p \leqslant p_c$, the distribution for $x = g/n$ is arbitrarily strongly peaked around $x = x^*$ in the thermodynamic limit, so that the system is self-averaging and the minimum gap x becomes the solution x^* of equation (49) with right-hand side zero (the $O(1/n)$ correction can be considered to obtain finite-size effects). The solution of (49) satisfies $(1-p) > x$, confirming the initial assumption.

The analytic results for the minimum gap for $p \leqslant p_c$ in the thermodynamic limit are given by the solution to (49) in the $n \to \infty$ limit. This solution is given in figure 7. For $p > p_c$ the gap is zero since the treatment of the regime $p > p_c$ shows (cf (25)) that $V(g)$ disappears beyond a tail extending out to $g = O(1)$, so that in the thermodynamic

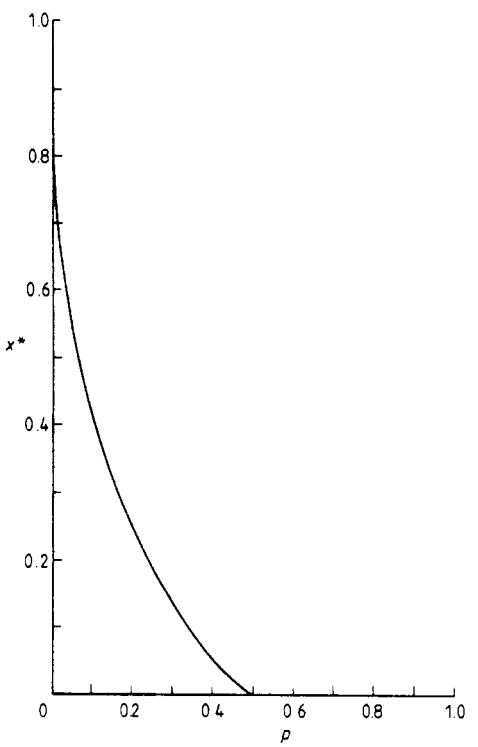

Figure 7. The order parameter x^* as a function of p found from the solution to (49).

limit, g/n is zero with probability 1. A comparison of the numerical curve of figure 4 with the analytic one of figure 7 confirms the correctness of the analytic approach and the high accuracy of the numerical calculations at large n.

The concentration dependence of the reduced gap in the most interesting regimes $p \sim p_c$ and $p \sim 0$ can be obtained analytically from (49) (in the thermodynamic limit, for $p \leq p_c$) with the results given below.

(a) $p \sim p_c$
From (49), x^* is zero at $p = p_c = 1/\alpha$. If

$$\varepsilon \equiv (p_c - p)/p_c \tag{51}$$

is small, x^* is also small, and satisfies (using (49))

$$x^*[\ln(\alpha - 1) - \ln x^* + 1] - \varepsilon + O(\varepsilon^2, (x^*)^2 \ln x^*) = 0. \tag{52}$$

Thus, in the critical region p just less than p_c, the reduced minimum gap is

$$x^* = \varepsilon/[1 + \ln(\alpha - 1) - \ln \varepsilon + O(\ln \ln(1/\varepsilon))]. \tag{53}$$

This shows that the critical exponent μ for the gap as defined above is exactly

$$\mu = 1 \tag{54}$$

confirming the conclusion from the numerical analysis. It also shows the presence of a logarithmic correction term.

(b) $p \sim 0$
Equation (49) gives $x^* = 1$ at $p = 0$. For small p,

$$\delta \equiv (1 - x^*) \tag{55}$$

is small, and the equation leads to

$$\delta \ln(p/\delta) + (\delta - p) + \ln \alpha + O(\delta^2, p^2) = 0. \tag{56}$$

Therefore

$$\delta = \ln \alpha/[\ln(\ln \alpha/p) - O(\ln \ln(1/p))] \tag{57}$$

which to leading order is

$$\delta \simeq -\ln \alpha/\ln p. \tag{58}$$

This explains the shape near $p = 0$ of the curves for $x^* = g/n$ (figures 4 and 7).

5. Conclusions

A new order parameter for percolative systems has been studied on Cayley trees. This quantity, the minimum gap, is of relevance in the study of dielectric breakdown in random media, as well as providing a new tool in the study of the geometric percolation problem. The Cayley tree calculations presented here give an exact solution for a case with a non-trivial percolation threshold. A summary of results we have found is as follows.

(i) The (reduced) minimum gap is a good order parameter on Cayley trees. Numerical and analytical results indicate that it self-averages in the thermodynamic limit, is finite below p_c and is zero above p_c.

(ii) A linearisation of the full Cayley tree equation (6) about $U = 1$ leads to results which are exact in the thermodynamic limit. The full behaviour of the order parameter in this limit is given (for $p \leqslant p_c$) by the solution to (49) (figure 7).

(iii) There are two critical behaviours present in the model: (*a*) as $p \to p_c$ the minimum gap goes to zero with exponent 1 and has logarithmic corrections (equation (53)), and (*b*) as $p \to 0$ the minimum gap becomes $x^* \sim 1 + \ln \alpha / \ln p$ (equations (57) and (58)).

Acknowledgments

PMD thanks Trinity College Oxford for support. PS thanks the Department of Theoretical Physics, Oxford for their hospitality during a stay in which this work was carried out.

References

Bowman D 1985 Private communication

Deutscher G, Zallen R and Adler J (ed) 1983 *Percolation Structures and Processess, Ann. Israel Phys. Soc.* vol 5 (Bristol: Adam Hilger)

Duxbury P M, Beale P D and Leath P L 1986a to be published

Duxbury P M, Shukla P, Stinchcombe R B and Yeomans J 1986b to be published

Fisher M E and Essam J W 1961 *J. Math. Phys.* **2** 609

Kantor Y 1985 *Proc. Geilo Conf. on Scaling Phenomena in Disordered Systems* (New York: Plenum)

Schuster H 1985 *Deterministic Chaos* (Mostbach: Physik Verlag)

Stauffer D 1979 *Phys. Rep.* **54** 1

—— 1985 *Introduction to Percolation Theory* (London: Taylor and Francis)

Stinchcombe R B 1974 *J. Phys. C: Solid State Phys.* **7** 179

—— 1983 *Phase Transitions and Critical Phenomena* vol 7, ed C Domb and J L Lebowitz (New York: Academic) p 151

Straley J 1977 *J. Phys. C: Solid State Phys.* **10** 3009